https://dx.doi.org/10.4314/dujopas.v10i2c.28
ISSN (Print): 2476-8316
ISSN (Online): 2635-3490
Dutse Journal of Pure and Applied Sciences (DUJOPAS), *Vol. 10 No. 2c June 2024*

Application of High-Resolution Aeromagnetic Data for Structural Frame Work of Zamfara Basement Complex, North Western Nigeria

[1*]A.M. Narimi, [2]A.A Rafiu & [3]U.D. Alhassan

[1]Department Applied Geophysics,
Federal University Birnin Kebbi,
Nigeria.

[2&3]Department of Geophysics,
Federal University of Technology,
Minna,
Nigeria

Email: amnarimi@gmail.com

Abstract

Zamfara state, located in the northwest of Nigeria, is regarded as one of the richest states in terms solid mineral abundance in Nigeria. Unofficial artisanal miners have found over 120 mining sites in the state. However, there is Insufficient knowledge of local and regional geology in the research area. High resolution aeromagnetic data were utilized to determine the depth of magnetic sources and basement tectonics. Clarifying the tectonic distribution of the basement complex and small portion of Sokoto sedimentary sequence within the research area is the aim of this investigation. Furthermore, this elucidation will help to differentiate the region's causative sources, which include contacts, faults, fractures, silk and dykes. Three approaches were compared for estimating the depth to magnetic sources namely: upward continuation, source parameter imaging, and Euler deconvolution. Euler deconvolution was upward continued to a distance of 1 km for (structural indexes 0 and 1, i.e., for contact and dyke) respectively. The map from these structural indexes exhibits similar patterns in terms of magnetic intrusive geological structures. Most magnetic structures and intrusive depth sources diminish at shallower range < 500 m while deeper sources > 1 km and 1.5 km were still present. The source parameter imaging produces the depth to the magnetic source, which ranges from 85.42 nT, which indicates a basement complex, to 1088.21 nT, which indicates a sedimentary basin. In addition to the subsurface geologic conditions, Visual inspection of the total horizontal derivative (THD), and tilt derivative (TD) revealed swift variations in the lithologic features and tectonic inferences as well as the subsurface geologic conditions. Three primary magnetic lithologic zones were identified from the analytical signal map classification: strong (> 0.051 nT/m), intermediate (0.016 to 0.051 nT/m), and low magnetic zones (< 0.016 nT/m). The lineament map, tilt derivative, and horizontal tilt derivative all showed the amplifications of various structural features (faults, fractures, and folds). These demonstrate the structural control of minerals in this research area.

Keywords: Structures, Mineralisation Zones, Correlation, Hydrothermal Alteration, Depth to Magnetic Sources.

Author for Correspondence

INTRODUCTION

The application of the magnetic technique in the geophysical exploration has become routine, as the method exploits the magnetic susceptibility to obtain lineaments, depth to magnetic sources, geologic boundaries, and geologic structures that reveal detailed features of mineralization (Bansal *et al*., 2011: Dentith & Mudge, 2014). Several Fourier filtrations processes such smoothing filters (upward continuation spectral analysis, source parameter imaging), sharpening filters (total horizontal derivative, vertical derivative, analytic signal) and geophysical transformation filters (reduction to pole and reduction to equator) are used to reveal the features of the map that are not likely to seen before the filtrations process (Augie & Ridwan 2021; Arewa and Fahad 2024).

Interpretation and enhancement of magnetic data are applied for delineating the deep and shallow geologic structures (Sharma, 1997). Moreover, the edge and texture detection allowed enhancing and identifying geologic contacts like lithologic boundaries and faults (Eldosouky *et al*., 2017).

Several researchers adopted edge detection techniques and smoothing filters in order to target geophysical signatures responsible for mineralization and hydrothermal alteration zones of the region. (Augie & Ridwan 2021; Arewa and Fahad 2024; Obaje *et al*., 2009; Kamba *et al*., 2016; Bonde *et al*., 2019). However, there is insufficient knowledge of local and regional geology in the research area. Different methods were used by researchers comes with conflicting figures which is usually due to wrong data analysis, for instant some researchers plot total magnetic intensity map without adding 33000 nT that was remove during data acquisition by fugro airborne services.in addition, the artisanal miners who make up the majority of the area's exploratory activities use a trial-and-error approach to exploring, which results in very little profit and the abandonment of mines and trenches that contribute to environmental degradation.

One of the primary objectives of this study are to use correlation between various techniques to determine the depth of magnetic structures and to use aeromagnetic data to identify the boundaries of anomalous zones within the Zamfara State Basement Complex. This will significantly increase the ability to derive geologic information from geophysical data, enhance the effectiveness and continuity of current edge detection approaches, reduce the impact of noise, while lowering the impacts of varied depth on the body and source dip.

The Study Area's Location and Geology

Zamfara state and some of its surroundings are included in this study. Latitudes 12°00'N and 13°00'N and longitudes 5°30'E and 7°00'E are within the study region, which covers an area of around six (6) half-degree aeromagnetic sheets. Geologically, The study area is supported by medium-coarse-grained quartz-mica schist, granite, migmatite, biotite, gneiss, diorite, biotite-hammelte granite, shale, phyllite and limestone . The location of the study region and its geology are shown in Figure 1. (Augie & Ridwan, 2021; Danbatta *et al*., 2008a).

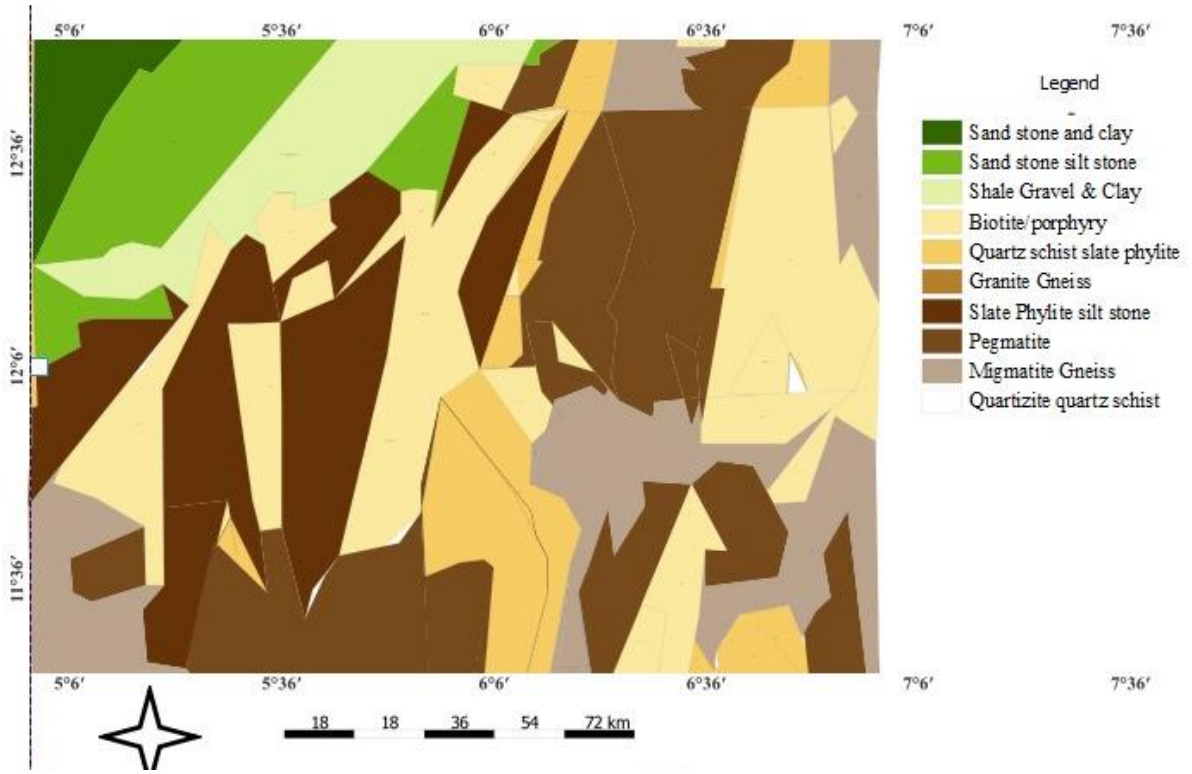

Figure 1: Location and Geology Map of the Study area modified after NGSA, (2006)

Upward Continuation:

The continuation integral arising from one of Green's theorems allows potential fields known at a set of points to be stated at adjacent higher or lower spatial locations in a source free zone (Blakely, 1995). The main applications of this notion are to decrease short-wavelength data noise by continuing the field higher and to adapt the altitude of observations to a datum as a tool for survey interpretation. By looking at the continuation operator in the wavenumber domain, it is possible to comprehend how the upward continuation process affects the fields. Equation (1) below gives the operator's form.

$$L(k) = e^{-|k|z} \quad (1)$$

where z is the continuation level of ground units, which is typically measured in meters, and |k| is the wavenumber, or equivalent to 2Πλ and λ, is the wavelength. The exponent's negative sign denotes an upward continuation (away from the field's sources).

Source parameter imaging (SPI)

The Source Parameter Imaging (SPI) function is a powerful technique for calculating the depth of magnetic sources (geometries, dip, susceptibility and density contrast (Kamba and Ahmed, 2017). Its accuracy has been shown to be +/- 20% in tests on real data sets with drill whole control (Ngozi *et al.*, 2019). While SPI is more user-friendly and produces a more comprehensive collection of coherent solution points, its accuracy is comparable to that of Euler deconvolution. A stated goal of the SPI method (Thurston and Smith, 1997) is that the resulting images can be easily interpreted by someone who is an expert in the local geology. Using both horizontal and vertical gradients, one may determine the local wave number (k) of the observed field for any point in a data grid. This method makes use of the link between source depth and k. When the source geometry is assumed (similar to the structural index in Euler deconvolution), the source depth at peaks in the local wave number grid is equal to n/k, where n = 1 for a contact and n = 2 for a dyke. Peaks in the wave number grid are identified

using a peak tracking algorithm (Blakely and Simpson, 1986) and valid depth estimates isolated. The Source Parameter Imaging method (Thurston and Smith, 1997) used in this work estimates the depth from the local wave number of the analytical signal. The analytical signal A1 (x, z) is defined by Nabighian (1972) as: The amplitude of the Analytic Signal in the 3-D given by: The amplitude of the Analytic Signal in the 3-D given by:$|A(x,z)|\sqrt{\left(\frac{\partial M}{\partial x}\right)^2+\left(\frac{\partial M}{\partial y}\right)^2+\left(\frac{\partial M}{\partial z}\right)^2}$ (2)

Where $\frac{\partial m}{\partial x}$, $\frac{\partial m}{\partial y}$ and $\frac{\partial m}{dz}$ are the gradients in x,y and z directions respectively.

$$K=\frac{\partial}{\partial x}tan^{-1}\left|\frac{\partial M}{\partial x}/\frac{\partial M}{\partial z}\right| \quad (3)$$

Euler deconvolution: The magnetic source's apparent depth is determined using Euler's homogeneity equation, which is obtained using Euler deconvolution. By using a "structural index" to represent the degree of homogeneity, this approach links the location of an anomaly's cause to the magnetic field and its gradient components. According to Daoui and Gabtni (2014), the structural index (SI) is a measurement of the field's fall-off rate with distance from the source. For magnetic data, Euler's homogeneity relationship can be expressed as follows:

$$(x-x_\circ)\frac{\partial T}{\partial x}+(y-y_\circ)\frac{\partial T}{\partial y}(z-z_\circ)\frac{\partial T}{\partial z}=N(B-T) \quad (4)$$

Where $\frac{\partial m}{\partial x}$, $\frac{\partial m}{\partial y}$ and $\frac{\partial m}{dz}$ is the location of the magnetic source at (x, y, z,) where total field (T) is detected. The local magnetic field is denoted by B. N, which is a measure of the magnetic field's fall-off rate, can be understood as the structural index (SI) (El Dawi, 2004).

Every solution that undergoes Euler deconvolution procedure entails choosing a suitable SI value and solving the problem for an optimal value using least-squares inversion. A square window size, or the number of cells in the gridded dataset to be used in the inversion at each chosen solution point, must also be supplied. All of the solution positions are in the center of the window. Euler's equation for solution depth, inversely weighted by distance from the window center, is solved using all of the window's points. In the whole field magnetic grid, the window should be big enough to encompass every solution anomaly of interest, but ideally not big enough to encompass any neighboring anomalies (Bansal *et al.*,2011).

METHODOLOGY

Acquired, compiled, and evaluated were high resolution aeromagnetic (HRAM) data sheets covering a portion of Zamfara state and its surroundings. These maps were acquired in 2009 as a part of the nationwide aerial survey that Fugro conducted under sponsorship from the Nigerian Geological Survey Agency (NGSA). The data were collected at a height of 80 meters along a 500-meter flight line spacing that was oriented in a NW-SE direction and a 2000-meter tie line spacing. The maps are half-degree sheets contoured mostly at intervals of 10 m, with a scale of 1:100,000. The International Geomagnetic Reference Field (IGRF) was used to eliminate the geomagnetic gradient from the data. The digitalized total magnetic intensity (TMI) data was subtracted from the estimated regional magnetic field to obtain the residual magnetic field which reflects local geological events.

RESULTS AND DISCUSSION

Below are the results of filters such Euler deconvolution, horizontal derivative, tilt derivative source parameter imaging, and analytical signal.

Euler deconvolution for determination of contact zones structural index = 0

Figure (4.1a, 4.1c and 4.1d) represent the Euler deconvolution for contact Structural Index SI = 0, Euler deconvolution upward continued to 1 km and 1.5 km respectively. The structural index is an exponential factor that indicates the pace at which the field decreases with distance from a source with a given shape. These aid in locating anomalous magnetic sources and their depths. Regarding the current inspection, it was reported that intrusive structures were found throughout the map, with the exception of the western axis, at shallower depths of less than 500 meters. Thus, the intrusive contact geological models were utilized. The Euler depth result indicates that the range of magnetic source depths is between 100 m, 200 m, 300 m, and 400 m. Figures 4.1c and 4.1d show the upward continuation of the Euler deconvolution to 1 km and 1.5 km, respectively. The majority of intrusive depth sources and shallow magnetic structures diminish in this region. Potential sources of mineralization in the western axis of the research area were estimated to be between 100 and 400 meters deep. The Euler deconvolution results, when compared to the Analytic signal map, likewise show that the high magnetic zone, high frequency, and high lineament density, respectively, are all associated with the shallow depth range (> 100 m).

Analytic Signal

The contact and dyke of Euler deconvolution (Figures 4.1b and 4.2b) show extremely comparable signatures with Analytic signal, thus the high and low magnetic signals in the vertical gradient are consistent with the high and low magnetic zones in the analytic signal, respectively. Granitic and metasedimentary rock assemblages could be the consequence of magmatic injections, which would explain the high magnetic signals. The edges of anomalous events, structural patterns, and lithological connections that depend on the magnetization of various rock compositions are displayed on the analytical signal map (Faruwa 2021). This allowed the entire study region to be divided into three main magnetic lithologic units: low magnetic zones (< 0.016 nT/m), intermediate (0.016 to 0.051 nT/m), and high (> 0.051 nT/m). Low frequency amplitude magnetic zones (LMZ) may correlate to sedimentary terrains made up of clay, pebbles, and sandstones, moderate magnetic zones (MMZ) may connect to younger metasediments, such as phyllites. While the main magnetic source outline, also known as the high magnetic zones (HMZ), is thought to be a dominantly intrusive zone that gives rise to granitic rocks (such as pegmatites, porphyritic granite, and biotite granite) and undifferentiated schists, granite gneiss, biotite gneiss, migmatite, and migmatite gneiss. (Fahad & Arewa, 2024).

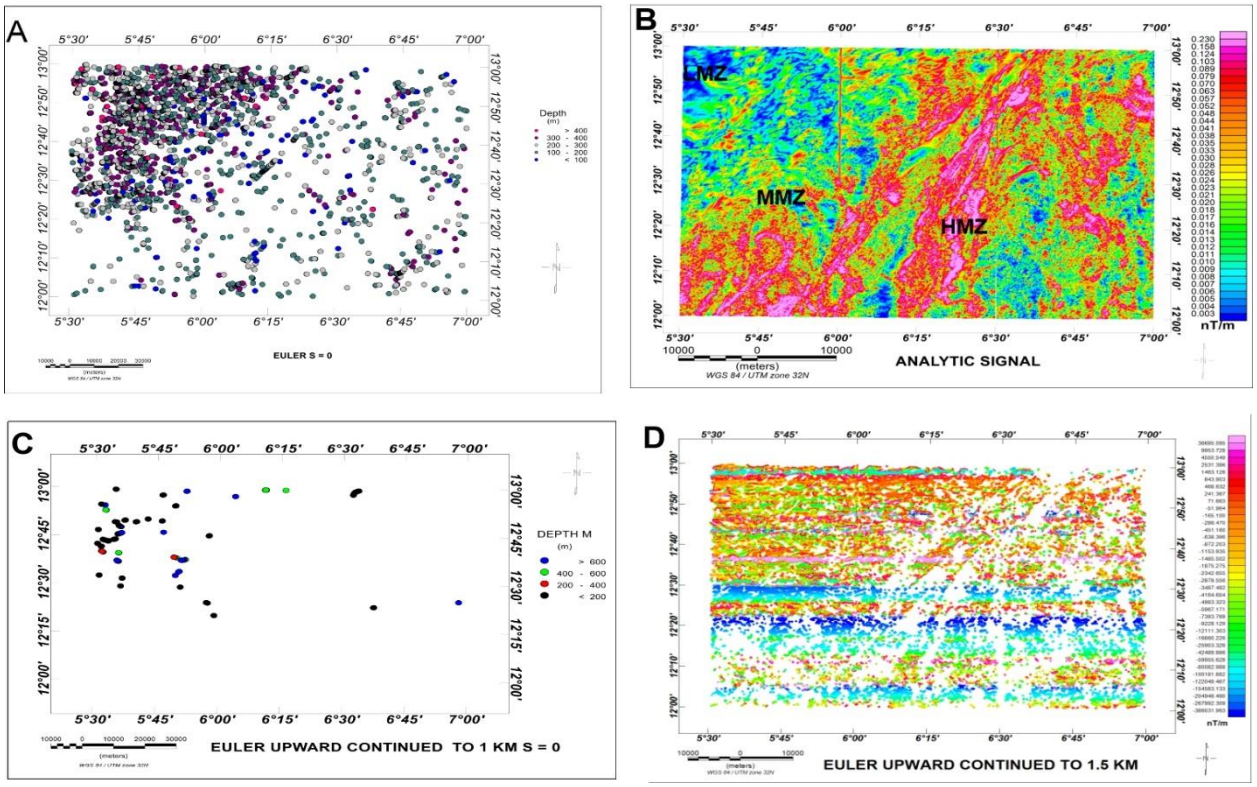

Figure 4.1a, 4.1b, 4.1c, and 4.1d showing Euler deconvolution at S = 0 for contact, Analytic signal, Euler deconvolution upward continued to 1 km and Euler deconvolution upward to 1.5 km respectively.

Euler deconvolution for determination of dykes at structural index = 1

Figure (4.2a, 4.2b and 4.2d) represent the Deconvolution using Euler for structural index SI = 1. for dyke. The contact and dyke exhibit similar patterns in terms of magnetic intrusive geological structures. The shallower depth of the magnetic sources are < 100 m and most of magnetic signatures diminishes and a depth greater 500 m except for the north eastern part of the study where deeper sources could be obtain. Euler deconvolution for dyke was also upward continued to 1 km and 1.5 km in figure 4.2c and 4.2d respectively. The map indicates that most magnetic structures and intrusive depth sources diminishes at shallower range < 500 m while deeper sources > 1 km and 1.5 km were still present. Potential sources of mineralization in the western axis of the research area were estimated to be between 100 and 400 meters deep. The Euler deconvolution results, when compared to the Analytic signal map, similarly show that the high magnetic zone, high frequency, and high lineament density, respectively, are all associated with the shallow depth range (<100 m).

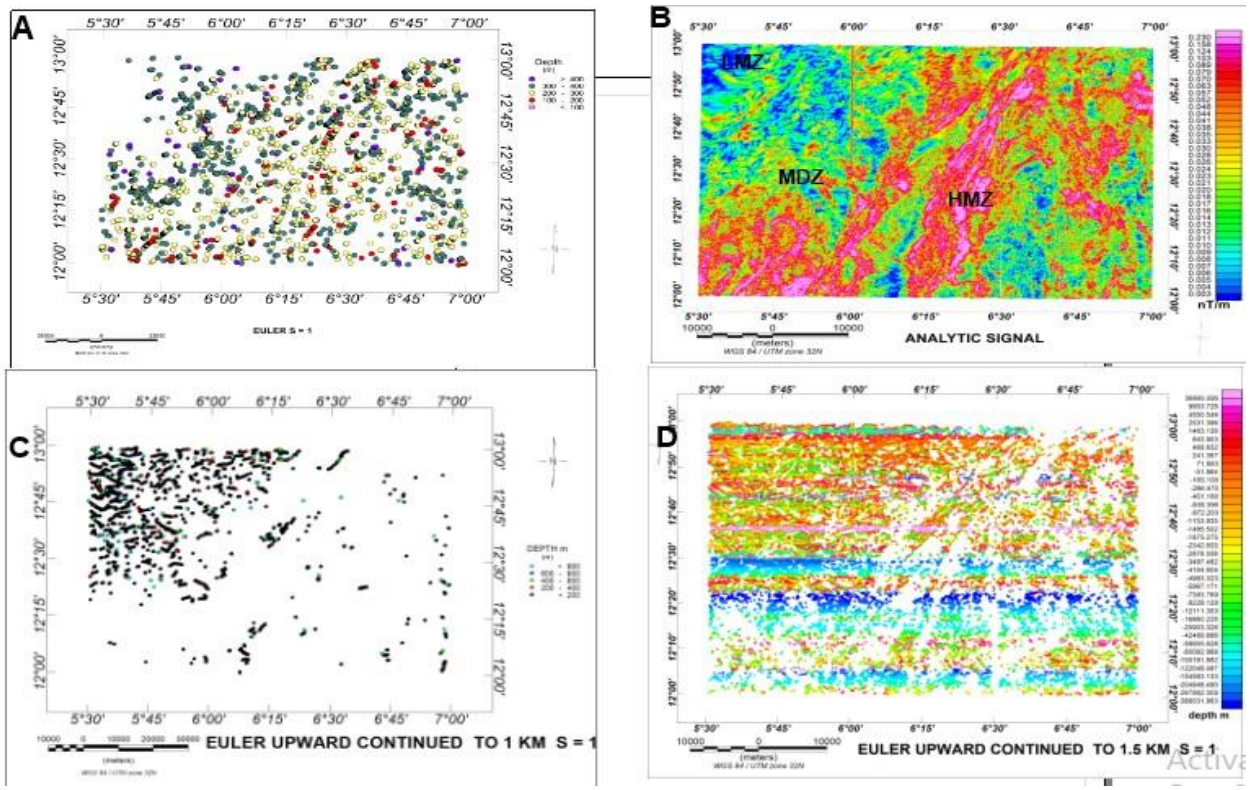

Figure 3a, 3b, 3c and 3d showing Euler deconvolution at S = 0 for contact, Analytic signal, Euler deconvolution upward continued to 1 km and Euler deconvolution upward to 1.5 km respectively.

Source Parameters Imaging

The source parameter imaging indicates a depth to the magnetic source of 85.42 m, which represents a basement complex, to 1088.21 m, which represents a sedimentary basin. The investigation area's northwest region has more sediment fill than the other areas shown on the map. This zone is indicated as Gandi sheet 30 and some part of Anka sheet 52, respectively. The source parameter imaging agrees with the geological map obtained from Nigerian Geological Survey Agency. Figure 1.

Lineament map

The lineaments map figure 4.3d can be divided into high frequency magnetic zones (HFMZ) and low frequency magnetic zones (LFMZ). High frequency (HFMZ) can be associated occasionally to dikes and silk intrusion in dolerite or granite which may also indicate that they are reversely magnetized (Fitches *et al*., 1985). HFMZ can also be associated with other structures such as fractures and faults. These structures can be from shallow crustal depth where pegmatites tend to be intruded along anisotropies (Brisbin, 1986). The low frequency magnetic zones (LFMZ) may represent sedimentary area where deeper sources could be obtained (Cerny, 1991c). The lineament map is well jointed mostly in N-E NW.

Horizontal tilt derivative **and Tilt derivative maps:**

The horizontal tilt derivative and Tilt derivative were displayed in Figures 4.3a and 4.3b, respectively. A similar structural trend was noted when comparing Figure 4.3a of the Tilt derivative map with Figure 4.3d of the Lineament map. The Tilt derivative map was categorized into two sections: low frequency, high wavelength anomalies and High frequency, short wavelength anomalies. It was observed that the short wavelength anomalies were concentrated in the northeastern and southcentral portions of the study area, indicating

a shallower depth of the causal sources in comparison to the other regions, where deeper source inferences could be made. Sources of narrow linear positive magnetic anomalies include fractures, dikes, sills and other major and minor faults were indicated from horizontal derivative map of the study area. These may indicate hydrothermal alteration zones, and structural elements associated with different mineralization of solid minerals in the area (Belgrano *et al.*, 2016). The horizontal tilt derivative, tilt derivative, and lineament maps all exhibit the amplifying mutations of these structural features (faults, fractures, and folds). These shows that minerals in the study area are structurally control. These structures could serve as a main conduit for hydrothermal activity may also indicate mineralization zones (Curewitz, & Karson, 1997).

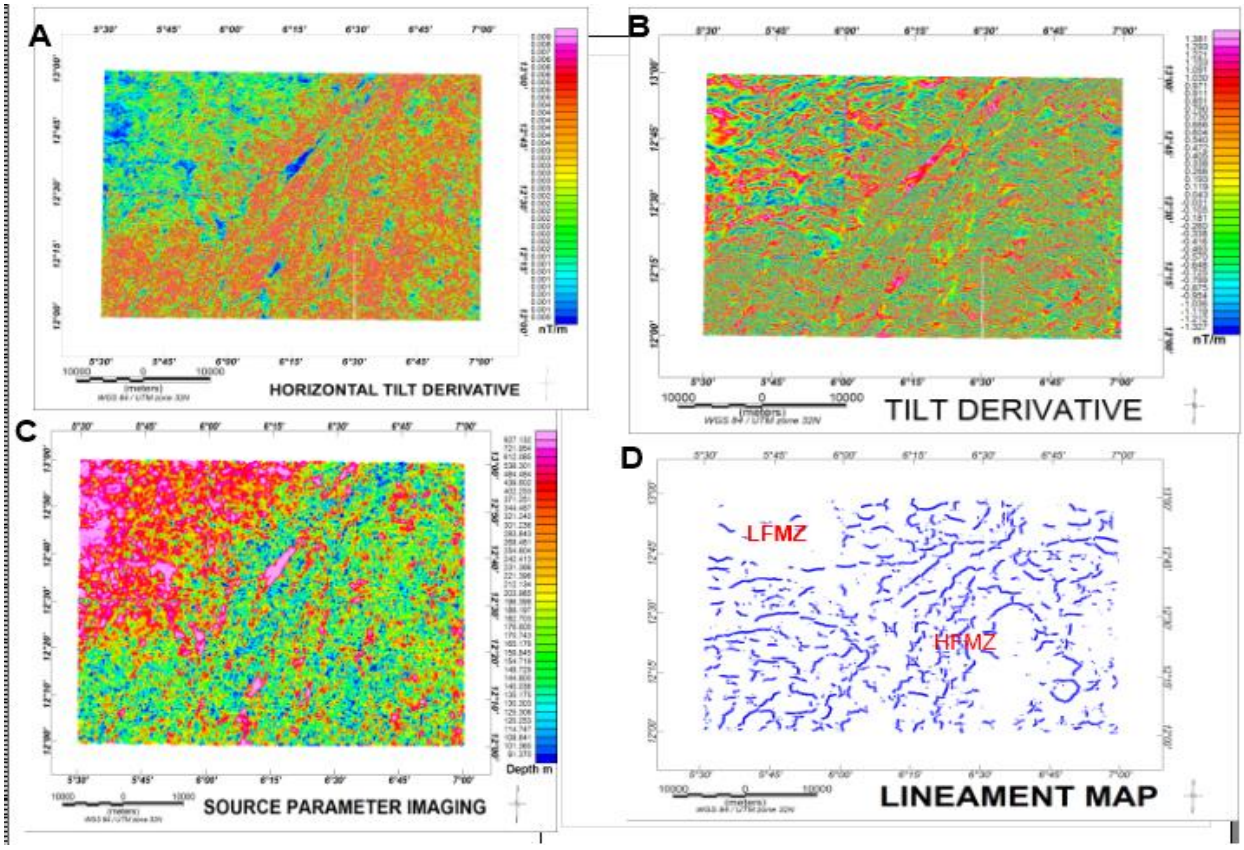

Figure 4.3a, 4.3b, 4.3c and 4.3d showing Horizontal tilt derivative, Tilt derivative, Source parameter imaging, and Lineament map respectively.

CONCLUSION

The study elucidated the tectonic implications pertaining to the distribution of basement complex zones and minor sedimentary sequence belts of Zamfara state and its environs. Fig. 4.1b, Fig. 4.3a and 4.3b (Analytic signal Map, Horizontal tilt derivative map and Tilt derivative map respectively) shows the structures that are responsible for harboring of economic minerals in the region. At the northeastern and northcentral and north southern part of area which is made up of basement complex that corresponds to Anka, Maru, Gummi, Gusau and Wonaka host magnetic minerals like Zinc, Aluminum, Copper Gold, Gemstone and granites. while the southern part which is made up of sedimentary rocks that corresponds to Dange,and Gandi host industrial minerals like limestone siltstone, shale, Clay and Sands. Furthermore, this study pinpointed causative sources, which include silk dykes, dykes, fractures, faults, and contacts in the region.

The vast majority of the magnetic minerals that are found in the study area are structurally control. Consequently, it is expected that lineaments discovered particularly trending north east and south west, could be home to the economic minerals indicated above. This is supported by the results of the filters employed in this study. If used effectively, these minerals might boost Nigeria's economy and open up economic opportunities that would create a large number of employment and ultimately end the country's poverty especially in the region.

REFERENCES

Arewa O. J., & Abubakar, F. (2024). Solid mineral potential evaluation using integrated aeromagnetic and aeroradiometric datasets. *Scientific Reports*, *14*(1), 1637.retrived from https://www.nature.com/articles/s41598-024-52270-6

Augie, A. I., & Ridwan, M. M. (2021). Delineation of Potential Mineral Zones from Aeromagnetic Data over Eastern Part of Zamfara. *Savanna Journal of Basic and Applied Sciences*, *3*(1), 60-66. Retrieved from http://www.sjbas.com.ng

Bansal A.R., Gabriel G., Dimri, V.P., & Krawczyk C.M. (2011). Estimation of depth to the bottom of magnetic sources by a modified centroid method for fractal distribution of sources: an application to aeromagnetic data in Germany, *Journal of Geophysics* 76, https://doi.org/10.1190/1.3560017. L11–L22.

Belgrano, T. M., Herwegh, M. & Berger, (2016). Inherited structural controls on fault geometry, architecture and hydrothermal activity: An example from Grimsel Pass, Switzerland. *Swiss. Journal of Geoscience.* 109, 345–364. DOI 10.1007/s00015-016-0212-9

Blakely R.J., Simpson R.W. (1986). Approximating edges of source bodies from magnetic or gravity anomalies. *Journal of Geophysics*, 51:1494-1498.

Blakely, R.J., (1995). Potential Theory in Gravity and Magnetic Applications. Cambridge: Cambridge University Press.

Bonde, D. S., Lawali, S., & Salako, K. A. (2019). Structural Mapping of Solid Mineral Potential Zones over Southern Part of Kebbi State Northwestern Nigeria. *Journal of Scientific and Engineering Research*, *6*(7), 229-240. *Available online www.jsaer.com*

Cordell, L., and Grauch, V.J.S., 1985. Mapping basement magnetization zones from aeromagnetic data in the San Juan basin, New Mexico. In *The utility of regional gravity and magnetic anomaly maps* (pp. 181-197). Society of Exploration Geophysicists.

Curewitz, D. & Karson A., (1997). Structural settings of hydrothermal outflow: Fracture permeability maintained by fault propagation and interaction. *Journal of. Volcanol. Geotherm. Res.* **79**, 149–168. https://doi.org/10.1016/S0377-0273(97)00027-9

Danbatta, U. A. (2008a). Precambrian crystal development in the northerwestern part of Zuru schist belt, northwestern Nigeria. *Journal of Mining and Geology*, *44*(1), 45-56.

Dentith, M., and Mudge, S.T. (2014). Geophysics for the Mineral Exploration Geoscientist, Cambridge University Press.

Dhaoui, M., & Gabtni, H. (2014). Depth to basement analysis from gravity field over the Guelb Ahmer horst (Ghadames petroleum province, Southern Tunisia, North Africa). *IOSR Journal of Applied Geology and Geophysics (IOSR-JAGG) vol*, *2*, 122-127. DOI: 10.9790/0990-025122127

El Dawi, M. G., Tianyou, L., Hui, S., & Dapeng, L. (2004). Depth estimation of 2-D magnetic anomalous sources by using Euler deconvolution method. *American Journal of Applied Sciences*, *1*(3), 209-214.

Eldosouky A.M., Abdelkareem M., Elkhateeb S.O. (2017). Integration of remote sensing and aeromagnetic data for mapping structural features and hydrothermal alteration zones

in Wadi Allaqi area, South Eastern Desert of Egypt. *Journal of African Earth Science* 130(2017):28–37

Faruwa, A. R. (2021). Airborne magnetic and radiometric mapping for litho-structural settings and its significance for bitumen mineralization over Agbabu bitumen-belt southwestern Nigeria. *Journal of African Earth Science.* 180, 104222. https://doi.org/10.1016/j.jafrearsci.2021.104222

Fitches W. R., Ajibade A. C., Egbuniwe, I. G., Holt R. W., & Wright J. B., (1985). Late Proterozoic Schist belts & Plutonism in NM Nigeria. *Journal of Geological Society of London,* 142: 319–337. https://doi.org/10.1144/gsjgs.142.2.0319

Kamba A.H., Ahmed S.K. (2017). Depth to Basement Determination Using Source Parameter Imaging (SPI) of Aeromagnetic Data: An Application to Lower Sokoto Basin, Northwest, Nigeria. *International Journal of Modern Applied Physics* 7(1):1-10

Lawal, T. O., (2020). Integrated aeromagnetic and aeroradiometric data for delineating lithologies, structures, and hydrothermal alteration zones in part of southwestern Nigeria. *Arab Journal of Geoscience.* **13**, 775 (2020). http://dx.doi.org/10.1007/s12517-020-05743-7

Nabighian M.N. (1972). The analytic signal of two-dimensional magnetic bodies with polygonal cross-section: Its properties and use for automated anomaly interpretation. *Journal of Geophysics* 37(3):507-517.

Nigerian Geological Survey Agency (2006). Aeromagnetic survey specification. Fugro Airborne Geophysical Survey. South Africa.

New Mexico. In Hinze, W.J. (ed.) The Utility of Regional Gravity and Magnetic Anomaly Maps. Tulsa: Society of Exploration Geophysicists, pp. 181–197.

Ngozi, A. O., Johnson, U. A., & Igwe, E. A. (2019). Spectral analysis and source parameter imaging of aeromagnetic data of Lafia and Akiri Areas, Middle Benue Trough, Nigeria. *International Journal of Physical Sciences*, 14(1), 1–14. doi:10.5897/ijps2018.4752

Obaje, N. G. (2009). *Geology & mineral resources of Nigeria.* Springer publishers, Germany. pp 1- 203.

Sharma P.V., (1997). Environmental and engineering geophysics. Cambridge University Press, Cambridge

Thurston J.B. Smith R.S., (1997). Automatic conversion of magnetic data to depth, dip, and susceptibility contrast using the SPITM method. Geophysics 62(3):807-813.